Chapter 3

MODEL APPROACHES AND INPUT DATA

This chapter is devoted to the description of modeling approaches to the assessment of long-range transport and contamination of the regions of the Russian North by Hg, PCBs and γ-HCH. The global character of these pollutants requires appropriate approaches to the assessment of their dispersion in the atmosphere. There are at least several reasons for the hemispheric or global consideration of the atmospheric pollutant dispersion. Firstly, volatile contaminants such as mercury and some POPs emitted to the atmosphere have essentially global atmospheric residence time estimated as long as months or even years and can be airborne transported practically over the whole globe [*Ebinghaus et al.*, 1999; *Vulykh and Putilina*, 2000]. Moreover, after being deposited to the Earth's surface these pollutants can be re-emitted to the atmosphere from areas situated far from traditionally considered industrial regions. Besides, the consideration of contamination of such remote regions as the Arctic at the hemispheric or global level seems to be reasonable.

Modeling approaches used in a number of studies of environment pollution by Hg, PCBs, and γ-HCH on the global or hemispheric scale are briefly outlined in Section 3.1. Following sections contain the description of the models developed at MSC-E. These models are based on the same atmospheric transport scheme. They are referred to three-dimensional Eulerian models. Therefore it is rather appropriate to talk about series of models describing transport of certain pollutants than about separate models. Nevertheless, the models contain peculiarities describing the behaviour of the mentioned pollutants in the compartments. Thus, mercury model more concentrated on complicated chemical transformations of mercury in the atmosphere, whereas POP model includes a developed description of persistent organic pollutants in the environmental compartments. The hemispheric model of mercury long-range transport (**MSCE-Hg-Hem**) is described in Section 3.2. The appropriate model for evaluation of hemispheric pollution by POPs (**MSCE-POP**) is presented in Section 3.3. To avoid duplication of description of common components the atmospheric transport scheme is described in detail only in for MSCE-Hg-Hem (Section 3.2) and just mentioned for MSCE-POP (Section 3.3). Instead, peculiarities of pollutant transformations and behaviour in the media are highlighted for both models.

The chapter also contains the description of input data required for the models. Meteorological data are described in Section 3.4. Information on land cover and leaf area index is presented in Sections 3.5 and 3.6 respectively. Section 3.7 contains a short description of data on air concentrations of chemical reactants. Data on ocean currents and sea ice are characterized in Sections 3.8 and 3.9.

3.1. Short review of modeling approaches used to the assessment of pollution by Hg, PCBs and HCHs on global/hemispheric scale

A great number of different studies of the Arctic pollution have been performed recently [*AMAP*, 1998]. Most of them were carried out using various measurement campaigns aiming at the investigation of contamination of the environment within this region. Only a few of them included the application of mathematical models. The application of modeling to the assessment of the environmental contamination recently takes on great significance. In spite of uncertainties in models and in the input information, model approaches are improved and become a useful tool for the investigation of dispersion and behaviour of contaminants in the environment. Modeling can complement the information on HM and POP content in different Arctic environmental compartments

obtained using measurement campaigns. In particular it can provide data on concentrations in air and other media with a certain spatial and temporal resolution. Modeling results can be used for the analysis of contamination pathways to the Arctic and for investigations of source-receptor relationship. Besides models can be used for the projection of contamination levels employing various emission scenarios. Here we would like to describe briefly some of them related to such chemicals as Hg, PCBs, and HCHs, which are of concern in this study.

Hg

The Danish Hemispheric Eulerian Model system (DEHM) was developed and recently applied to estimate the transport of mercury to the Arctic. The earlier version of the model was used in AMAP phase I [*AMAP*, 1998], and the model has been described in several papers (e.g. *Christensen* [1997, 1999]; *Barrie et al.* [2001]). The modeling system includes a meteorological model based on the PSU/NCAR Mesoscale Model version 5 (MM5) [*Grell et al.*, 1995] and a 3-dimensional air pollution model DEHM. The description of chemical transformations of mercury is based on the scheme from the GKSS model [*Petersen et al.*, 1998]. In the present version there are 13 mercury species in the gaseous, aqueous and particulate phase. The model includes the parameterization of springtime mercury depletion events in the Arctic atmosphere. It is assumed that during the Arctic polar sunrise the oxidation rate affecting the transformation of Hg^0 to HgO increases by 25% in the boundary layer over sea ice under sunny conditions. Dry deposition velocities of the reactive gaseous mercury species are determined on the basis of the resistance method. For wet deposition of reactive and particulate mercury simple scavenging coefficient different for in-cloud and sub-cloud scavenging is applied [*Christensen*, 1997]. The model was used for the simulation of mercury long-range transport and deposition for the period from October 1998 to December 2000 on the basis of the new global inventory of mercury emissions for 1995 on a $1^o x 1^o$ grid [*Pacyna and Pacyna*, 2002], which includes mercury speciation. No re-emission from land and oceans is considered in the model. As the initial concentration and boundary conditions the concentration of 1.5 ng/m^3 of Hg^0 is used. The model results suggest that mercury depletion events in the Arctic atmosphere are of an essential importance. The total deposition of mercury in the area north to the Polar Circle is increased from 78 to 181 tonnes per year in model runs without and with depletion parameterization.

Another model used for the simulation of mercury species in the gaseous and aqueous phase is a Eulerian Multiscale Global/Regional Atmospheric Heavy Metals Model (GRAHM) developed at Canadian Meteorological Centre (CMC). The development of this model was started from an operational weather forecasting model Global Environmental Model (GEM) [*WMO*, 2000]. The model is based on solving a set of dynamic equations for all meteorological processes and includes a description of mercury species chemical transformations in the atmosphere. The mercury chemical scheme is adapted from G.*Petersen et al.* [1998]. For the description of contamination mass conserving 3-D quasi-monotonic semi-Lagrangian mass conserving scheme is employed. The discretization in time is based on the two-time-level semi-Lagrangian scheme. The model is capable to use variable resolution in vertical as well as in horizontal direction. Therefore it can operate with different scales and can produce both global distribution of mercury concentrations in the atmosphere and high-resolution regional concentration fields. The model was applied to simulation of global mercury distribution using emission inventory of anthropogenic mercury sources for 1990 of GEIA [*Pacyna et al.*, 1996]. However, this inventory does not contain information on mercury speciation, vertical distribution of emissions and point sources.

Another approach to the identification of sources of Canadian High Arctic pollution by total gaseous mercury (TGM) is based on the 10-day back trajectory cluster analysis and the potential source contribution function (PSCF) model [*Lin et al.*, 2001]. To investigate the long-range transport and source-receptor relationship of atmospheric pollutants a receptor model called PSCF has been developed. Using the combination of chemical measurements and computed backward trajectories of

air parcels to the points of observations (receptor sites), the PSCF model is capable to identify potential sources and pathways of a pollutant. Along with this model the cluster analysis of backward trajectories was applied to analyze the regional transport patterns and to project possible sources of pollutants. On the base of these techniques the study of potential sources and dominant pathways of Canadian High Arctic pollution by mercury was performed using the 1995 TGM concentrations measured at Alert site. The 10-day backward trajectories were computed by the trajectory model HYSPLIT4. According to the results of the study the long-range transport events occur only in the cold seasons. The potential source regions are located in Eurasia, Northern America and Europe. During the Arctic summer elevated TGM concentrations can be caused by the exchange of volatile mercury between the air and the underlying surface.

PCBs and HCHs

A simple global two-dimensional model for studying the fate of organochlorines in the environment is presented in [*Strand and Hov*, 1996]. This paper describes the application of the developed model to the simulation of α and γ-HCH distribution in three environmental compartments: atmosphere, soil and seawater. Only the most important processes are included into this multicompartment model. These are the transport within the atmosphere, wet deposition with precipitation, exchange with sea and soil compartments, sedimentation and degradation. The model was used to study the distribution of α– and γ-HCH with the use of data for the period 1960-1989. The results show that in spite of the coarse resolution and a certain level of simplification the model is able to reproduce reasonably well the observed atmospheric and oceanic levels of HCHs. It was shown that the major part of emitted HCH (92%) was partitioned to the ocean compartment due to its very significant capacity. From this amount 21% was contained in the surface waters and 71% - in deep waters.

The application of a global-scale multicompartment transport model to the evaluation of environmental fate of pesticides (hexachlorocyclohexanes) is presented in [*Koziol and Pudykiewicz*, 2001]. The model developed permits to give a realistic representation of interaction between such environmental compartments as the atmosphere, hydrosphere, cryosphere, and soil system. Along with the atmospheric part it includes the simulation of exchange between the air and the underlying surface (water, soil, snow, and ice). The atmospheric transport is described on the basis of equations in a general contra variant form. The terrain following spherical coordinate system is chosen with horizontal resolution 2° x 2°. The model includes the soil module for simulation of diffusion and convection of a pollutant within the soil. The computations were based on two-year meteorological data of Global Reanalysis data set for 1993-1994, climatological data, and estimations of HCHs' application during the simulated period. The computed concentrations were compared with observations made in the high Arctic at sites Alert, Ny-Alesund, Dunai, and Tagish. The comparison indicates that the results of the model are in a good agreement with measured air concentrations and their trends. According to the modeling results India seems to be the most significant source of pollution by HCHs. Other potential sources of HCHs can be located in Central Europe, the Ukraine, North Africa, and Mexico.

The fugacity-based mass balance model was developed to determine the global distribution of selected persistent organic pollutants [*Wania and Mackay*, 1999]. The global environment is represented in the model as the 10 latitudinal bands or climatic zones each of which is divided into a set of well-mixed compartments, namely, the atmosphere, land, freshwater and seawater. It includes transport and exchange processes between these compartments, degradation, partitioning of chemicals between the gaseous and particulate phase in air, as well as between the dissolved phase and suspended matter in water. This version of the model has no vertical division of the atmospheric compartments and processes of advection and diffusion. Air temperatures and exchange rates between atmospheric compartments are defined as seasonally varying parameters. The model

developed was applied to simulation of α-HCH global distribution [*Wania et al.*, 1999]. Based on this simulation seasonal variations and long-term trends of α-HCH concentrations in the atmosphere and ocean water were assessed. The model reproduced the latitudinal dependence of measured α-HCH concentrations in air and reversible air-sea exchange for the period 1960-1996. Differential persistence of chemicals in different climate zones and temperature-controlled partitioning between the atmosphere and the underlying surface were indicated as the most significant factors for the global distribution of HCHs. The model results suggest that the most part of applied α-HCH was degraded within the soil compartment where it was used and a small fraction was transferred to the terrestrial and marine environment of the Arctic region via the atmosphere and rivers. However even this small amount can result in elevated levels of HCH concentrations in this area. The most important sources of the Arctic pollution by this chemical were temperate and boreal climatic zones. The Arctic Ocean can be the final sink for the α-HCH where it is accumulated and degraded with the half-life of about ten years.

The updated version of the model was also used in the study of the global historical fate of PCBs [*Wania*, 1999]. The modifications include vertically layered representation of the atmosphere, a forest canopy compartment, and some other improvements of parameterization of the processes. The simulation was based on the estimates of emission of seven PCB isomers into the global environment from 1930 to 2000. It was assumed that the chemical composition of these emissions was constant throughout the considered period and all the release of PCBs occurred to the atmosphere. The results are of a preliminary character they are deviating within an order of magnitude in comparison with measurements. Based on the model results it was obtained that the total amount of seven PCBs released during the period of 1930-2000 was distributed within the environment in the following way: 64% was degraded, 18% was transported to the deep sea and 1% was buried in fresh water sediments, and 17% was dispersed within various environmental compartments. The analysis of congeneric composition of PCBs in different media suggests that the polar atmosphere is represented by lighter congeners and their amount there tends to increase with time. It was concluded that there is a need to perform computations for individual PCB chemicals rather than for the chemical mixture with average properties since the simulated fate of various congeners is different to a significant extent. It was indicated that even relatively minor fractions of the global PCB emissions being transported northward result in elevated levels of the PCB concentrations in the polar region.

The approaches used in these studies and their results were carefully studied prior to set up investigations in the framework of this project. To achieve the goals of the present study the dynamic Eulerian hemispheric models were considered to be suitable for the evaluation of pathways and spatial distribution of contamination in different environmental compartments and to provide estimates of source-receptor relationships. The description of models developed for this study is presented below in this chapter.

3.2. MSCE-Hg-Hem model

The scheme of model treatment of main mercury processes in the atmosphere is presented in Figure 3.1. Mercury enters the atmosphere from anthropogenic and natural sources. They include point (coal-fired power plants, waste incinerators, volcanoes etc.) and diffuse area sources (mill tailings, municipal wastes, geologically enriched soils) [*Jackson*, 1997; *Gustin et al.*, 1999]. Whereas anthropogenic emissions contain a number of mercury species (elemental mercury vapour, oxidized gaseous and particulate mercury), natural emissions mostly consist of elemental vapour. Moreover, mercury vapour is emitted to the atmosphere from the sea surface due to marine biota activity [*Kim and Fitzgerald*, 1986]. Detailed description of mercury emission sources is presented in Chapter 4.

Once emitted to the atmosphere mercury is transported through it with the air masses (advective transport) and dispersed by eddy diffusion. During the pathway in the atmosphere mercury species undergo physical and chemical transformations resulting in their mutual redistribution. Thus, elemental mercury is oxidized by such oxidants as ozone and *OH* radical. Besides, it is dissolved in cloud water and takes part in aqueous-phase oxidation and reduction reactions, formation of sulphite and chloride complexes, which are in turn adsorbed by soot particles. The model chemical scheme is described in detail in Section 3.2.2. Mercury species are removed from the atmosphere by means of surface uptake and precipitation scavenging. The model parameterization of dry and wet deposition processes is considered in Section 3.2.3.

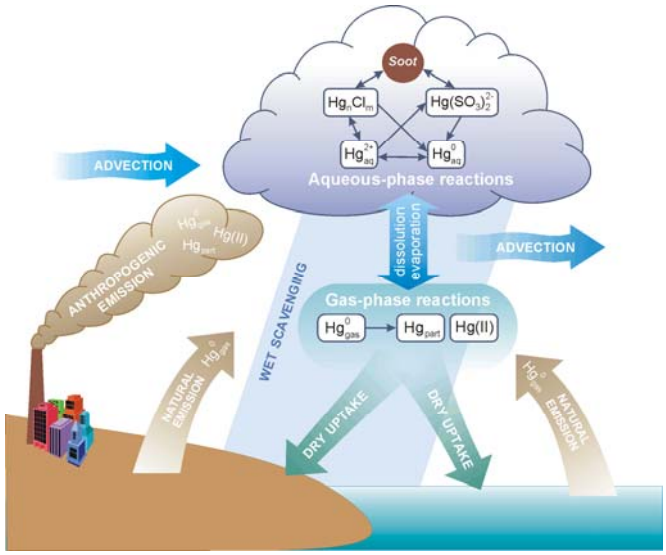

Figure 3.1. *The model scheme of mercury behaviour in the atmosphere*

The model computation domain covers the whole Northern Hemisphere with spatial resolution 2.5° both in zonal and meridional directions. The surface grid structure of the model domain is shown in Figure 3.2. To avoid a singularity at the pole point, peculiar to the spherical coordinates, the grid has a special circular mesh of radius 1.25° including the North Pole. In the vertical direction the model domain consists of eight irregular levels of terrain-following sigma-pressure (σ-p) coordinate defined as a ratio of local atmospheric pressure to the ground surface pressure [*Jacobson*, 1999]. The vertical grid structure of the model is presented in Figure 3.3.

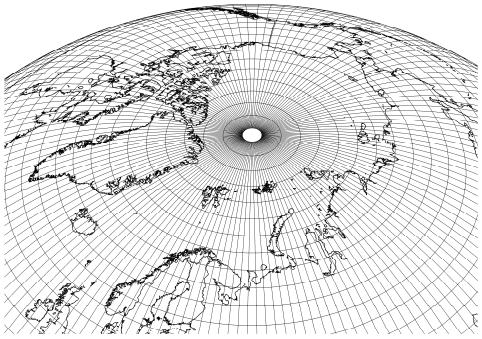

Figure 3.2. *Horizontal grid structure of the model domain. Geographical coordinates with 2.5° × 2.5° resolution and the pole grid cell*

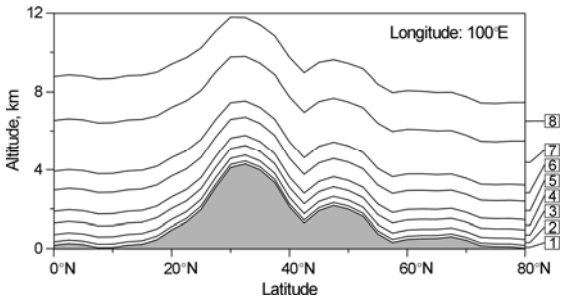

Figure 3.3. *Vertical grid structure of the model domain. Eight terrain-following σ-levels: 1 – σ = 0.99; 2 – 0.96; 3 – 0.91; 4 – 0.85; 5 – 0.77; 6 – 0.68; 7 – 0.55; 8 – 0.4*

3.2.1. Atmospheric transport

The model description of mercury atmospheric transport is based on the three-dimensional advection-diffusion equation adapted to the (σ–p) coordinate [see e.g. *Jacobson*, 1999]:

$$\frac{\partial}{\partial t}(q_i p_s) = -\nabla_H \cdot (q_i p_s \mathbf{V}_H) - \frac{\partial}{\partial \sigma}(q_i p_s \dot{\sigma}) + \frac{\partial}{\partial \sigma}\left[K_z \frac{g^2 \rho^2}{p_s^2} \frac{\partial}{\partial \sigma}(q_i p_s) \right] + C_i + S_i - R_i \qquad (3.1)$$

Here $q_i = c_i / \rho$ is mixing ratio of i^{th} mercury species;

c_i and ρ are the mercury species volume concentration and the local air density;

$\sigma = d\sigma / dt$ is the vertical scalar velocity in the σ–p coordinate;

∇_H and $\mathbf{V}_H$ denote vectors of horizontal divergence operator and horizontal wind velocity respectively;

K_z is the vertical eddy diffusion coefficient; and g is the gravitational acceleration.

In Eq. (3.1) we omitted horizontal components of eddy diffusion because of the coarse horizontal grid resolution. The local air density ρ is coupled with air temperature T_a and surface pressure p_s through the equation of state:

$$\rho = \frac{\sigma p_s}{R_a T_a}, \qquad (3.2)$$

where R_a is the humid air gas constant.

The first two terms on the right hand side of Eq. (3.1) describe horizontal and vertical advection of a pollutant in the atmosphere. The third term represents vertical eddy diffusion, the fourth considers species mutual chemical transformations (C_i), and the last two terms describe bulk pollutant sources (S_i) and removal processes (R_i). Eq. (3.1) is solved by means of the time-splitting technique [*Yanenko*, 1971; *Marchuk*, 1975; *McRae et al.*, 1982]. Following this method, Eq. (3.1) is decomposed into several separate sub-equations describing different physical and chemical processes, which are solved successively during each time step.

Advection

In spherical coordinates the sub-equation of Eq. (3.1) describing horizontal advection has the following form:

$$\frac{\partial}{\partial t}(q_i p_s) = -\frac{1}{R_E \cos\varphi}\left[\frac{\partial}{\partial \lambda}(q_i p_s V_\lambda) + \frac{\partial}{\partial \varphi}(q_i p_s V_\varphi \cos\varphi) \right] \qquad (3.3)$$

where λ and φ are the geographical longitude and latitude;

R_E is the Earth radius;

V_λ and V_φ are zonal and meridional components of the wind velocity respectively.

Moreover, the former term in the square brackets describes the zonal advective transport, while the latter term represents the meridional one.

Eq. (3.3) is numerically solved using Bott flux-form advection scheme [*Bott*, 1989a; 1989b]. This scheme is mass conservative, positive-definite, monotone, and is characterized by comparatively low artificial diffusion [see e.g. *Dabdub and Seinfeld*, 1994]. In order to reduce the time-splitting error in strong deformational flows the scheme has been modified according to [*Easter*, 1993]. The original

Bott scheme has been derived in the Cartesian coordinates. To apply the scheme to the transport in spherical coordinates it has been modified taking into account peculiarities of the spherical geometry. Detailed description of the Bott advection scheme in the spherical coordinates is presented in [*Travnikov*, 2001].

The vertical advection part of Eq. (3.1) is written as follows:

$$\frac{\partial}{\partial t}(q_i p_s) = -\frac{\partial}{\partial \sigma}(q_i p_s \dot{\sigma}) . \tag{3.4}$$

This one-dimensional advection equation is solved using the original Bott scheme generalized for a grid with variable step $\Delta\sigma$.

Vertical velocity

The very important issue for any air quality model is the mass consistency. It means that supplied wind and air density fields (surface pressure p_s is a full analog of air density in σ-p coordinate system) should satisfy the continuity Eq. (3.5):

$$\frac{\partial p_s}{\partial t} + \nabla_H \cdot (p_s \mathbf{V}_H) + \frac{\partial}{\partial \sigma}(p_s \dot{\sigma}) = 0 . \tag{3.5}$$

In the terms of an air quality model it implies that the model maintain a uniform mass mixing ratio field of an inert tracer [*Odman and Russel*, 2000]. It is exactly realized only if the air quality model and a meteorological model supplying input data have the same *discretization*, i.e. grid structure, time step, and finite-difference formulation. However, many transport models (including considered one) have discretization different from that used in the data supplying meteorological model. Besides, time resolution of the meteorological data (6 hours for the model involved) is often considerably lower than the model time resolution defined by the stability condition (15-45 minutes). It requires temporal interpolation of the meteorological data. All mentioned above can lead to a considerable mass inconsistency and the uniform tracer field cannot be maintained. To adjust input meteorological fields to the model discritization vertical wind velocity $\dot{\sigma}$ is calculated from the continuity Eq. (3.5) at each step using the procedure similar to that suggested in [*Odman and Russel*, 2000].

Since the non-linear advection scheme is used for vertical advection, it is difficult to derive the vertical velocity directly from Eq. (3.5). Instead one can solve Eq. (3.5) using exactly the same procedure as for Eq. (3.3) and (3.4) for one time step and equate the obtained value of surface pressure to that interpolated from the input data. As a result for each vertical column of the computation domain we obtain system of non-linear equations:

$$p_s = F_k(\dot{\boldsymbol{\sigma}}) \quad k = 1, \ldots, N. \tag{3.6}$$

Here $\dot{\boldsymbol{\sigma}} = (\dot{\sigma}_1, \ldots, \dot{\sigma}_N)$ is the vector of vertical wind velocities at the upper boundaries of σ-layers;

N is the number of the layers.

Solving the Equations system (3.6) for $\dot{\boldsymbol{\sigma}}$ at each vertical column and taking into account boundary condition at the surface $\dot{\sigma}_0 = 0$ we obtain field of vertical wind velocities. We apply standard FORTRAN library MINPACK (http://www.netlib.org/minpack/) for the solution of the non-linear Equations system (3.6).

Eddy diffusion

Vertical eddy diffusion is described by the following equation:

$$\frac{\partial}{\partial t}(q_i p_s) = \frac{\partial}{\partial \sigma}\left[K_z \frac{g^2 \rho^2}{p_s^2} \frac{\partial}{\partial \sigma}(q_i p_s) \right]. \qquad (3.7)$$

Vertical eddy diffusion coefficient $K_z = K_z(\lambda,\varphi,\sigma)$ is supplied by the atmospheric boundary layer module of the meteorological data preparation system (see Annex C). Non-linear diffusion Eq. (3.7) has been approximated by the second-order implicit numerical scheme in order to avoid restrictions of the time step caused by possible sharp gradients of species mixing ratio $q_i(\sigma)$. The obtained finite-difference equation is solved by means of the sweep method.

Initial and boundary conditions

The model computation domain has two boundaries: upper and equatorial. Long residence time of mercury in the atmosphere requires setting appropriate initial and boundary conditions to take into account mercury contained in the computation domain before the computations and the input fluxes of mercury through the boundaries.

According to the numerous measurements carried out for last decades [e.g. see *R.Ebinghaus et al.*, 1999] elemental mercury Hg^0 is more or less uniformly distributed over the Northern Hemisphere (background concentrations are around 1.7 ng/m^3). Vertical distribution of Hg^0 is also rather uniform [*Banic et al.*, 1999]. Therefore we prescribed uniform distribution of elemental mercury concentration at the upper boundary – 0.185 pptv (corresponding to about 1.5 ng/m^3 at 1 atm and 20°C). On the other hand, some gradient of total gaseous mercury (TGM) was observed over the ocean between the Northern and Southern Hemispheres [e.g. see *Banic et al.*, 1999]. According to *R.Ebinghaus et al.* [2001] mean concentrations of TGM over the Northern and Southern Hemispheres are 1.7 and 1.3 ng/m^3 respectively. Elemental mercury makes up the main part of TGM. Summarizing the measurement data from [*Slemr*, 1996] we set the gradient of Hg^0 to 0.05 ng/m^3/degree at the equatorial boundary. Since the residence time of other mercury species in the atmosphere is considerably shorter we neglected their input through the boundaries. Currently, only atmospheric module is adequately developed for the mercury transport description. Therefore, the lower boundary at the Earth surface is closed. The mercury fluxes through the lower boundary are indirectly considered by deposition and “natural emission and re-emission” processes.

To fill up the model domain with mercury from anthropogenic sources of different regions and continents (it is necessary for the inter-continental transport assessment) we performed a computation run for the period of one year without any boundary and initial conditions. Then we used the obtained concentrations of mercury species as initial conditions for the regular computation run. Besides, the contribution of different sources to mercury incoming through the upper boundary is assumed to be the same as at the highest atmospheric layer.

3.2.2. Atmospheric chemistry

The overview of main physical and chemical processes of mercury transformation in the atmosphere is given in Section 2.1. The current model parameterization is mostly based on the chemical scheme developed by *G.Petersen et al.* [1998]. In order to adjust the original scheme for global long-term calculations it was simplified taking into account only the most important reactions [*Ryaboshapko et al.*, 1999]. Fast irreversible reactions were assumed to be instantaneous, while reversible ones were

replaced by appropriate equilibrium conditions. Besides, up-to-date ideas of mercury atmospheric chemistry were also represented.

Mercury occurs in the atmosphere in various forms in gaseous, aqueous, and solid phase, which are undergo numerous physical and chemical transformations. The model considers the following mercury forms: gaseous elemental Hg^0_{gas}, gaseous oxidized Hg(II) (mostly $HgCl_2$); particulate oxidized Hg_{part}; and four liquid phase forms - elemental dissolved Hg^0_{aq}, mercury ion Hg^{2+}_{aq}, sulphite complex $Hg(SO_3)^{2-}_2$, and aggregate of chloride complexes Hg_nCl_m. The main mercury transformations in the atmosphere are schematically described in the Figure 3.4

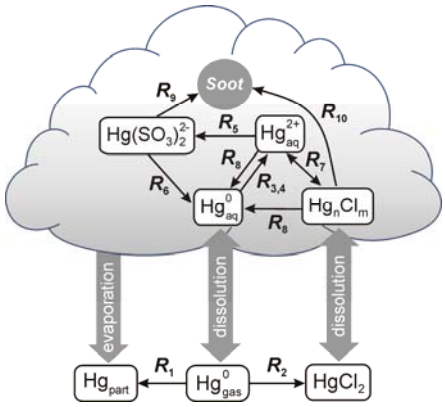

Figure 3.4. *Scheme of physical and chemical transformations of mercury in the atmosphere*

Gaseous phase

One of the most important gas phase reactions is oxidation of elemental mercury by ozone (R_1):

$$Hg^0_{gas} + O_3 \rightarrow Hg(II)_{part} + products \tag{3.8}$$

Since, ozone is always in plenty under ordinary atmospheric conditions this second-order reaction is described by a first-order rate expression with the reaction rate constant depending on the reactant concentration:

$$R_1 = -\frac{d[Hg^0_{gas}]}{dt} = k'_1[Hg^0_{gas}], \tag{3.9}$$

$$k'_1 = k_1[O_3]_{gas}, \quad k_1 = A\exp(-E_a/(R_{univ}T))$$

where A = 2.1·10^{-18} cm^3/(molec·s); E_a = 10.36 kJ/mole; R_{univ} = 8.31 J/(mole·K); and ozone concentration $[O_3]_{gas}$ is in molec/cm^3 [*Hall,* 1995].

It is believed that the product of the reaction is particulate mercury (see Section 2.1.2). Monthly mean fields of ozone concentration over the whole Northern Hemisphere were taken from [*Wang et al.*, 1998] and then adapted to the model grid (see Section 3.7).

Gas phase oxidation of elemental mercury by chlorine can be noticeable in the ocean boundary layer during night time (R_2):

$$Hg^0_{gas} + Cl_2 \rightarrow HgCl_2(gas) \tag{3.10}$$

with the reaction rate expression:

$$R_2 = -\frac{d[Hg^0_{gas}]}{dt} = k'_2[Hg^0_{gas}] \tag{3.11}$$

$$k'_2 = k_2[Cl_2]_{gas},$$

where k_2 = 3.7·10^{-18} cm^3/(molec·s) and chlorine concentration $[Cl_2]_{gas}$ is in molec/cm^3.

We adopted air concentrations of chlorine in the atmosphere suggested by *C.Seigneur et al*. [2001] described in Section 3.7. Although chlorine concentrations are low (about 100 ppt) in comparison with those of ozone, it could make up considerable contribution to oxidation of elemental mercury due to high reaction rate constant (Eq. 3.11).

Another possible significant oxidant is hydroxyl radical. Its influence on mercury oxidation could be comparable with that of ozone. However, because of absence of reliable data on the reaction rate constant (see Section 2.1.2) we did not include it into the scheme.

Aqueous phase

In the cloud environment elemental gaseous mercury Hg^0_{gas} is dissolved in cloud water (see Fig. 3.4). This process is described by equilibrium conditions with Henry's law constant (non-dimensional) depending on the air temperature (Eq. 2.1).

Dissolved elemental mercury Hg^0_{aq} is oxidized by ozone producing mercury oxide *HgO*, which is very short-lived in the liquid phase and is rapidly transformed to the mercury ion Hg^{2+}_{aq} (R_3). Thus, the resulting reaction can be written as follows:

$$Hg^0_{aq} + O_3 \rightarrow Hg^{2+}_{aq} + products\,, \tag{3.12}$$

with the reaction rate expression:

$$R_3 = -\frac{d[Hg^0_{aq}]}{dt} = k'_3[Hg^0_{aq}]\,; \tag{3.13}$$

$$k'_3 = k_3 H_{O3}[O_3]_{gas}\,,$$

where $k_3 = 7.8\cdot10^{-14}$ (molec/cm^3)$^{-1}$s^{-1}, ozone concentration $[O_3]_{gas}$ is in molec/cm^3.

This reaction rate constant is derived from values presented in Table 2.2 taking into account equilibrium conditions of ozone dissolution in cloud water. Temperature dependence of non-dimensional Henry's low constant H_{O3} for ozone is described by Eq. 2.4.

Elemental mercury in aqueous phase is also oxidized by dissolved chlorine $Cl(I)_{aq}$ with formation of mercury ion Hg^{2+}_{aq} (R_4):

$$Hg^0_{aq} + Cl(I)_{aq} \rightarrow Hg^{2+}_{aq} + products\,.$$

Reaction rate expression for this reaction has the following form:

$$R_4 = -\frac{d[Hg^0_{aq}]}{dt} = k'_4[Hg^0_{aq}]\,; \tag{3.14}$$

$$k'_4 = k_4 H_{Cl2}[Cl_2]_{gas}\,,$$

where $k_4 = 3.3\cdot10^{-15}$ (molec/cm^3)$^{-1}$s^{-1}, chlorine concentration $[Cl_2]_{gas}$ is in molec/cm^3, non-dimensional Henry's low constant H_{Cl2} is presented in Table 2.1.

Mercury ion Hg_{aq}^{2+} reacts in the solution with sulphite ions SO_3^{2-} resulting in the formation of mercury sulphite complex $Hg(SO_3)_2^{2-}$ (R_5) [*Petersen et al.,* 1998]:

$$Hg_{aq}^{2+} + 2SO_3^{2-} \rightarrow Hg(SO_3)_2^{2-} . \tag{3.15}$$

The reaction rate is determined by the air concentration of SO_2 and the cloud water *pH* (see Table 2.3):

$$R_5 = -\frac{d[Hg_{aq}^{2+}]}{dt} = k_5'[Hg_{aq}^{2+}] ; \tag{3.16}$$

$$k_5' = k_5[SO_2]_{gas}^2 \cdot 10^{4pH} ,$$

where $k_5 = 1.8 \cdot 10^{-42}$ (molec/cm^3)$^{-2}$s^{-1}, and $[SO_2]_{gas}$ is in molec/cm^3.

The sulphite complex $Hg(SO_3)_2^{2-}$ is dissociated to mercury sulphite $HgSO_3$, which is unstable, and is readily reduced to Hg_{aq}^0. Thus, the reduction process (R_6) can be described as:

$$Hg(SO_3)_2^{2-} \rightarrow Hg_{aq}^0 + products \tag{3.17}$$

with the reaction rate expression:

$$R_6 = -\frac{d[Hg(SO_3)_2^{2-}]}{dt} = k_6[Hg(SO_3)_2^{2-}] , \tag{3.18}$$

where $k_6 = 4.4 \cdot 10^{-4}$ s^{-1}.

This process increases the amount of dissolved elemental mercury in a droplet hampering further dissolution of gaseous mercury. Hence, the scheme implies negative feedback controlling elemental mercury uptake from the air.

Mercury ion Hg_{aq}^{2+} also takes part in a number of reactions leading to the formation of various chloride complexes Hg_nCl_m (R_7). These reversible reactions in the first approximation can be replaced by equilibrium concentrations of free mercury ions and mercury in the aggregate of chloride complexes ([$HgCl^+$], [$HgCl_2$], [$HgCl_3^-$], [$HgCl_4^{2-}$]). The equilibrium ratio of the appropriate mercury concentrations depends upon water content of chloride ion $[Cl^-]$ and is defined as follows [*Lurie*, 1971]:

$$r_1 = \frac{[Hg_nCl_m]_{aq}}{[Hg_{aq}^{2+}]} = \frac{[Cl^-]_{aq}}{1.82 \cdot 10^{-7}} + \frac{[Cl^-]_{aq}^2}{6.03 \cdot 10^{-14}} + \frac{[Cl^-]_{aq}^3}{8.51 \cdot 10^{-15}} + \frac{[Cl^-]_{aq}^4}{8.51 \cdot 10^{-16}} . \tag{3.19}$$

Besides, aqueous chemistry includes reduction of divalent mercury $Hg(II)_{aq}$ (both mercury ion Hg_{aq}^{2+} and chloride complexes Hg_nCl_m) in reaction with hydroperoxy radical $HO_2^{\bullet}$ (R_8):

$$Hg(II)_{aq} + HO_2^{\bullet} \rightarrow Hg_{aq}^0 + products \tag{3.20}$$

The appropriate reaction rate has the following expression:

$$R_8 = -\frac{d[Hg(II)_{aq}]}{dt} = k'_8[Hg(II)_{aq}]\,; \qquad (3.21)$$

$$k'_8 = k_8 H_{HO2}[HO_2^{\bullet}]_{gas}\,,$$

where $k_8 = 2.8\cdot10^{-17}$ (molec/cm^3)$^{-1}$s^{-1}, hydroperoxy radical concentration $[HO_2^{\bullet}]_{gas}$ is in molec/cm^3.

Monthly mean fields of concentration of hydroperoxy radical over the whole Northern Hemisphere were taken from [*Spivakovsky et al.*, 2000] and then adapted to the model grid (see Section 3.7). Temperature dependence of non-dimensional Henry's low constant H_{HO2} for hydroperoxy radical is taken from [*Jacobson*, 1999]:

$$H_{HO2} = 4.89\cdot10^4 \exp\left[6639.4\left(\frac{1}{T}-\frac{1}{298}\right)\right]. \qquad (3.22)$$

Sulphite and chloride complexes can be adsorbed and desorbed by soot particles in the aqueous phase (R_9, R_{10}). Comparatively fast equilibrium of these two reverse processes can also be described by means of "dissolved-to-adsorbed ratio". Based on the appropriate reaction rates it could be taken equal to 0.2 in both cases [*Petersen et al.,* 1998]:

$$r_2 = \frac{[Hg(SO_3)_2^{2-}]_{aq}}{[Hg(SO_3)_2^{2-}]_{soot}} = \frac{[Hg_nCl_m]_{aq}}{[Hg_nCl_m]_{soot}} = 0.2\,. \qquad (3.23)$$

As it was mentioned above one can distinguish three groups of mercury compounds being in equilibrium. The first group (*A*) contains elemental mercury in the gaseous and dissolved phase; the second one (*B*) consists of the mercury sulphite complex both dissolved and on soot particles; and the third group (*C*) includes free mercury ions, dissolved mercury chloride complexes and those on soot particles and gaseous mercury chloride:

$$\begin{aligned} A &= Hg^0_{gas} + Hg^0_{aq}\,;\\ B &= \left\{Hg(SO_3)_2^{2-}\right\}_{dis} + \left\{Hg(SO_3)_2^{2-}\right\}_{soot}\,; \qquad (3.24)\\ C &= Hg^{2+}_{aq} + \left\{Hg_nCl_m\right\}_{dis} + \left\{Hg_nCl_m\right\}_{soot} + \left\{HgCl_2\right\}_{gas}\,. \end{aligned}$$

According to this simplified scheme and introduced notations mercury transformations in the liquid phase are described by the following system of the first-order differential equations:

$$\begin{cases} \dfrac{d[A]}{dt} = -\alpha k'_2[A] + \beta k_4[B] + k'_5\delta[C],\\ \dfrac{d[B]}{dt} = -\beta k_4[B] + \gamma k'_3[C], \qquad (3.25)\\ \dfrac{d[C]}{dt} = -\gamma k'_3[C] + \alpha k'_2[A] - k'_5\delta[C]. \end{cases}$$

Here $\alpha = H_{Hg}L_w / (1 + H_{Hg}L_w)$ is the fraction of mercury in the *A* group corresponding to the dissolved form, and L_w is the non-dimensional liquid water content defined as volume of cloud water per unit volume. Parameter $\beta = r_2 / (1 + r_2)$ denotes mercury fraction of the *B* group in the dissolved phase.

Value $\gamma = r_2 r_3 / (r_2 r_3 + r_1 r_3 + r_1 r_2)$ is the fraction of mercury in the *C* group corresponding to the mercury ion Hg^{2+}_{aq}, whereas $\delta = \gamma(1+r_1)$ is fraction of divalent mercury $Hg(II)_{aq}$ in C group. Parameter $r_3 = H_{HgCl2} L_w / (1 + H_{HgCl2} L_w)$ is the fraction of mercury chloride $HgCl_2$ in cloud water. The analytical solution of the equations system with appropriate initial conditions defines mercury evolution in the aqueous phase during one time step.

The non-dimensional liquid water content L_w is evaluated according to parameterization suggested in [*Hongisto*, 1998]. It is equal to 10^{-7} for clouds without precipitation; $3 \cdot 10^{-7}$ for the large-scale cloudiness with precipitation; and 10^{-6} for the convective cloudiness with precipitation. Cloud cover data for the two types of cloudiness (large-scale and convective) is provided by the meteorological data preparation system (Annex C).

Mercury Depletion Events

Taking into account general ideas and review of the literature (see Section 2.1.3) on Mercury Depletion Events phenomenon (MDE) we adopt the following assumptions for the model parameterization.

1. We assume that MDE can occur only over open seawater areas, which were previously covered with ice during winter period. We exclude a possibility of penetration of *BrO* precursors through ice cover. Hence, we think that MDE can take place over coastal zones of the Arctic Ocean. Only those grid cells are taken into account, which cover both land and sea.

2. We suppose that the water surface was previously covered with ice if air temperature in a given point was permanently lower than -3°C during wintertime (assumed seawater freezing point). Then in springtime the temperature became higher than 0°C, and ice melting started. Besides, during springtime ice-drift becomes more intensive and areas of open water appear. Conditionally we "switch on" the MDE module if air temperature during previous 24 hours was higher that 0°C. We understand the conventional character of such a "trigger" because open water can appear at low negative temperatures.

3. We assume that total duration of MDE during springtime in any point does not exceed 4 weeks and MDE takes place every day (instantly at noon) during this period. The MDE module can be "switched on" only within the period from April to June.

4. We believe that during the MDE concentration of elemental mercury near the surface layer drops down from its usual level to 0.1 ng/m^3. Oxidation of Hg^0 leads to the formation of RGM (50%) and Hg_{part} (50%). The oxidized products are partly scavenged from the atmosphere within a given modeling grid cell, partly transported outside it and scavenged later.

5. We accept that the MDE covers the lowest 1 kilometre height layer of the atmosphere. Within this layer the intensity of the phenomenon linearly decreases with height to zero at the top of the layer. Hence, during the MDE elemental mercury has rising profile from 0.1 ng/m^3 at the surface to its usual values at 1 km height. Contrary, oxidized forms have dropping profile from their maximum at the surface to their usual values at 1 km height.

We took the Arctic definition accepted within the AMAP programme (Fig. 3.5). It covers the terrestrial and marine areas north of the Arctic Circle, north of 62°N in Asia and 60°N in North America, modified to include the marine areas north of the Aleutian chain, Hudson Bay, and parts of the North Atlantic Ocean including the Labrador Sea.

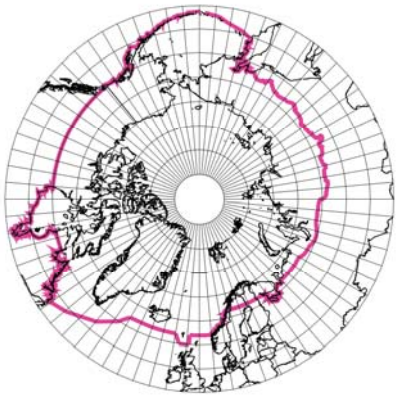

Figure 3.5. *AMAP Arctic area [AMAP, 1998]*

3.2.3. Removal processes

Mercury is removed from the atmosphere due to dry uptake of particulate and gaseous species by the underlying surface and through the scavenging of both the gas-phase and aqueous forms with precipitation. Appropriate sub-equation of Eq. (3.1) describing removal processes of i^{th} species is as follows:

$$\frac{\partial q_i}{\partial t} = -(\Lambda_i^d + \Lambda_i^w + \Lambda_i^{aq})q_i \tag{3.26}$$

where Λ_i^d, Λ_i^w, and Λ_i^{aq} are the rates of dry, wet deposition and removal of the aqueous phase respectively.

Since surface pressure is not changed in this processes, we have divided both parts of the original equation by p_s. All the removal processes are considered in the model successively.

Dry deposition

Particular mercury as well as some gaseous species is removed from the atmosphere through the contact with the underlying surface. They approach the ground surface (soil, rocks, vegetation, water etc.) due to advection, diffusion or sedimentation processes and stick to or react with it. This process is described by a part of Eq. (3.26) referred to the surface level:

$$\left.\frac{\partial q_i}{\partial t}\right|_{surf} = -\left.\Lambda_i^d q_i\right|_{surf} \tag{3.27}$$

where the rate of dry deposition (uptake) Λ_i^d is proportional to dry deposition velocity V_d^i:

$$\Lambda_i^d = V_d^i \left(\frac{g\sigma}{R_a T_a}\right)_{surf}. \tag{3.28}$$

Here subscript *surf* denotes values related to the ground surface. It should be noted that the expression in the parenthesis characterizes transformation from Cartesian to (σ-p) coordinate system and equals to inverse absolute value of the Jacobian ($J = -R_a T_a / g\sigma$).

In the current version of the model we apply a simplified parameterization of the dry deposition velocity for aerosol particles developed in [*Pekar*, 1996]. This approach is based on measured deposition velocities [*Sehmel*, 1980] as functions of aerosol size (*d*), roughness of the underlying

surface (z_0) and friction velocity parameter (u_*). Reasoning from the analysis of scientific literature (see Section 2.1) it is adopted that mercury particle-carriers have characteristic mass median diameter d = 0.7 μm and dry deposition velocities of particulate mercury are described by the following formulas:

$$V_d^{part} = \begin{cases} (0.02u_*^2 + 0.01)(z_0 10^3)^{0.33}, & \text{land} \\ 0.15u_*^2 + 0.013, & \text{sea} \end{cases}$$

here V_d^{part} is in cm/s, z_0 in m, and u_* in m/s.

Currently, only two types of underlying surface are distinguished in the parameterization of dry deposition of particulate mercury (land and seawater surface). It is proposed to introduce specification of dry deposition on different types of land cover (forests, grassland, deserts etc.)

Dry deposition velocity of gaseous oxidized mercury *Hg*(II) is taken the same as for nitric acid V_d^{oxid}=0.5 cm/s due to similarity of their properties [*Petersen et al.*, 1995]. This parameter does not vary seasonally and with different type of the underlying surface.

Dry uptake of elemental gaseous mercury Hg^0_{gas} by various types of underlying surface is not adequately defined yet. Some experts [*US EPA*, 1997] suppose that this type of mercury removal is not an essential sink on a regional and global scale. It is assumed that absorption of Hg^0_{gas} by vegetation takes place only if its concentration exceeds so-called “compensation point” (about 20 ng/m^3). It implies that the absorption is realized only in the immediate vicinity of emission sources [*Lyon et al.*, 1999]. According to another viewpoint [*Lin and Pehkonen*, 1999] dry uptake of elemental mercury is considered to be the dominating mechanism of mercury removal from the atmosphere. *T.Bergan and H. Rodhe* [2001] also note that elemental mercury uptake is an important mechanism of the global mercury cycle, but it is poorly considered in the literature.

Summarizing available literature data [*Travnikov and Ryaboshapko*, 2002] we adopt the following parameterization of the process. There is no dry uptake of elemental gaseous mercury by water surface and land surface not covered by vegetation. It is also absent during nighttime. Over the vegetated surface during daytime dry uptake velocity has the following form:

$$V_d^{gas} = \begin{cases} 0\ , & T_s \le T_0 \\ A_d \dfrac{T_s - T_0}{T_1 - T_0} \cos\theta_s\ , & T_0 < T_s \le T_1 \\ A_d \cos\theta_s\ , & T_s > T_1 \end{cases}$$

here T_s is the surface temperature, T_0 = 273 K and T_1 = 293K;

A_d is equal to 0.03 cm/s for forests and 0.01 cm/s for other vegetation types;

θ_s is the solar zenith angle calculated according to [*Jacobson*, 1999].

Wet scavenging

Scavenging of aerosol particles and soluble gases by precipitation is one of the most effective mechanisms of mercury removal from the atmosphere. First of all it concerns particulate Hg_{part} and gaseous oxidized *Hg*(II) mercury forms. Wet scavenging rate Λ_i^w in Eq. (3.26) is proportional to precipitation intensity $I_p(\sigma)$ and can be roughly approximated by the following expression:

$$\Lambda_i^w = W_i I_p(\sigma) \left(\frac{g\sigma}{R_a T_a} \right)_{surf} \frac{(q_i I_p)_{surf}}{\int q_i I_p(\sigma) d\sigma} \tag{3.29}$$

where W_i is the washout ratio of the i^{th} species defined as a ratio of the species concentration in precipitation to the concentration in the surface air.

The last ratio in (3.29) takes into account variation of precipitation intensity with altitude. This approach is aimed at fitting simulated concentration in precipitation of scavenged species to measured ones using empirical values of the washout ratios W_i.

It is assumed that presence of *Hg* does not affect properties of a particle with respect to wet scavenging (it make up only a minor part of the particle mass). Instead, wet scavenging of particles mainly depends on their size distribution spectrum. Both Hg_{part} [*Milford and Davidson*, 1985] and $SO_4^=$ [*Whitby*, 1978; *Schryer*, 1982; *Kiehl and Brieglep*, 1993, *Weiss et al*., 1977] are accumulated in sub-micron size mode (0.1 – 1 μm). Allen et al. [2001] also demonstrated that more than 50% of Hg_{part} mass is settled on particles with diameter below 1 μm. Therefore, the value of washout ratio peculiar to sulphate particles $W_{part} = 5 \cdot 10^5$ [*Iversen et al.*, 1989] was adopted for the parameterization of Hg_{part} wet removal. Washout ratio of gaseous oxidized mercury is taken to be equal to that of nitric acid $W_{oxid} = 1.4 \cdot 10^6$ [*Petersen et al.*, 1995; *Jonsen and Berge*, 1995].

Aqueous phase removal

All aqueous-phase mercury species are scavenged from the atmosphere by precipitation with the removal rate:

$$\Lambda_i^{aq} = \frac{g\sigma}{R_a T_a} \frac{\Delta I_p}{L_w \Delta\sigma} \tag{3.30}$$

where ΔI_p is the increment of precipitation within a grid cell. It is taken to be zero for negative values.

All aqueous-phase species scavenged by precipitation during its falling down return back to the atmosphere in the particulate form if precipitation is entirely evaporated before the ground.

3.3. MSCE-POP model

This chapter contains a description of the current version of the MSCE-POP model, which was employed for calculations of PCB and γ-HCH transport over the Northern Hemisphere. This model is multicompartment 3-dimensional, and includes descriptions of POP behaviour in different environmental media (atmosphere, soil, seawater, vegetation, sea ice and snow), incorporated as different program modules. Spatial resolution of the model is 2.5x2.5° except for the seawater and ice/snow modules, which operate with resolution 1.25x1.25°. The following sections give a detailed description of these modules as well as a general structure of the model.